An optical fiber sensor for detecting laser-induced plasma shock waves

Chen Jianping, Ni Xiaowu, Lu Jian, Bian Baomin, Wang Yawei
(Department of Applied Physics, Nanjing University of Science and Technology, Nanjing, 210094)

Abstract: We have recently developed an optical fiber sensor based on beam deflection for detecting shock waves. It successfully measured the changing rate of the refractive index of the transient airborne shock waves produced by plasmas in laser material damage processes. This measurement system, particularly suitable for instantaneous detection of axisymmetrical shock waves, is broadband as well as non-contact.

Key words: laser plasma shock wave optical fiber sensor

用于探测激光等离子体冲击波的光纤传感器

陈建平 倪晓武 陆 建 卞保民 王亚伟
(南京理工大学应用物理系, 南京, 210094)

摘要: 利用探测光束通过轴对称流场时的偏折效应, 设计了一种光纤传感器, 并用于探测激光对材料破坏过程中在空气中激发的等离子体冲击波, 获得了探测位置处激光等离子体冲击波流场折射率随时间的变化率。该方法适用于轴对称流场的瞬态测试, 具有宽带和非接触的特点。

关键词: 激光等离子体 冲击波 光纤传感器

Introduction

The generation of a shock wave in the ambient gas is a well-known phenomenon in the laser material damage process, during which the ambient air near the laser focal spot subjects to the great pressure of the explosion of laser-induced plasma[1~5]. Such a shock wave, in some reports[6,7], is termed as laser plasma shock wave (LPSW). The research on the generation and attenuation process of the LPSW contributes to our understanding of the laser material damage process and mechanism.

A broadband microphone or piezo-electric transducer (PZT) may be one of the most sensitive and convenient devices available for detecting airborne ultrasonic pulses. We can calibrate it easily, and read the pressure of ultrasonic waves directly. Though its bandwidth is not broad enough to detect the shock waves generated by high power laser pulses with duration of nanoseconds, the PZT may be positioned at a distance where the LPSWs have attenuated to ultrasonic pulses[6]. An ultrasonic optical fiber sensor based on birefringence, which can respond linearly to ultrasonic pulses as high as 30MHz, may have enough bandwidth for detecting the LPSWs[8~10]. However, it has poor sensitivity. Furthermore, it distorts the shock wave fields for it is a contact method. High-speed photography and transient optical interferometry[1] are the two non-contact methods for shock wave detection. They can measure the shock wave speed quantitatively and visualize its profile. Although interferometers are highly sensitive to weak shock waves,

they suffer from stability, mobility and calibration problems. It is also difficult to interpret interferograms involving shock waves. Moreover, we cannot locate the generating position of the shock wave with the interferogram because of the intense flash of the plasma. Based on knife-edge beam deflection[11], another non-contact system for measuring the shock wave field can be constructed. It can only detect the intense shock wave near the focal spot with low sensitivity.

In this paper, a single-mode optical fiber, being used to replace the knife-edge as the position-sensitive detector, not only retains its desirable wide band characteristic, but also exhibits high sensitivity. With the fiber shock wave sensor, the changing rate of the refractive index in the shock wave field has been determined experimentally.

1 Principle

Generally, when a laser pulse with a power density greater than 10^8 W/cm^2, irradiates a solid target, the target material will successively melt, evaporate, and become plasma. The plasma sharply explodes at an initial speed up to 10^7 cm/s[1] into the ambient air with a high pressure, which induces a shock wave. This shock wave propagates at an ultrasonic speed at first and attenuates quickly to the local sound speed within a certain distance. Supposed that the plasma is a point source, the refractive index of the shock wave field will have a spherically symmetrical characteristic[2,12]. If a thin collimated optical beam passes through the shock wave field, it deflects slightly away from its original direction at an angle β, caused by the sharp increase of the refractive index of the shock wave front. It will be demonstrated that if the variation of the deflection angle with time is known experimentally, then the changing rate of the refractive index of the shock wave field can be determined correspondingly.

1.1 Experimental detection of the deflection angle

The schematic diagram of the presented detection system is shown in Fig. 1. The target is put flatly at axis x, and the YAG laser pulse normally irradiates the target at origin O along axis y. After passing through the shock wave field, the He-Ne detection beam (at the wavelength of 632.8nm) is focused on a single-mode fiber end (with a core diameter of 4μm) by a microscope objective ($20^{\times}$) with focal length f = 4mm. Because of the shock wave, the focal spot at the fiber end shifts from its original position by a distance $d = f \tan\beta \approx f\beta$, where β is the small deflection angle. The fiber coupling intensity I of the optical beam is

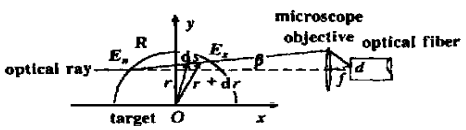

Fig. 1 Diagram of LPSW detection

$$I = I_0 \exp(-d^2/w_0^2) \approx I_0 \exp[-(f\beta)^2/w_0^2] \tag{1}$$

where I_0 is the maximum coupling intensity of the fiber, and w_0, the width of the focal spot on the fiber end, can be given as following

$$\frac{1}{w_0^2} = \frac{1}{w^2}\left(1-\frac{1}{f}\right)^2 + \frac{1}{f^2}\left(\frac{\pi w}{\lambda}\right)^2 \tag{2}$$

where w is the detection beam waist, and λ is the wavelength.

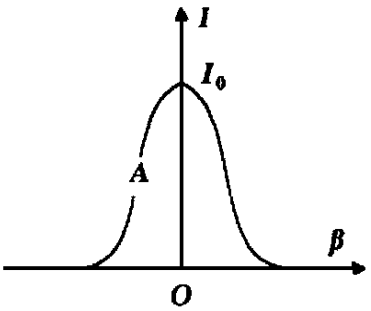

Fig. 2 Coupling intensity versus deflection angle

Hence the coupling intensity I varies with deflection angle β, according to a Gaussian function, as shown in Fig. 2. For optimum performance the fiber should be aligned so that the initial coupling intensity is half of I_0, say, at the point A in the intensity curve as shown in Fig. 2. Thus we ensure that the detection system works at a linear area with the highest sensitivity. Therefore, the Eq. (1) can be simplified as

$$I \approx -0.833 f I_0 \beta / w_0 \tag{3}$$

Hence the deflection angle β can be easily measured from the detection of the coupling intensity as $\beta = kI$ (4)

where k is a system constant, and $k = -w_0/(0.833 f I_0)$.

1.2 Determination of the refractive index changing rate

According to the ray equation of geometrical optics[13,14] $\frac{\mathrm{d}}{\mathrm{d}s}\left(n\frac{\mathrm{d}\boldsymbol{r}}{\mathrm{d}s}\right) = \nabla n$ (5)

where $\boldsymbol{r}$ is the direction vector from the origin to the point (x, y), and s is the distance along the detecting light ray (see Fig. 1). It can be seen that β equals the y component of $(\mathrm{d}\boldsymbol{r}/\mathrm{d}s)$ at the exit point of the shock wave field E_x. Integrating the y component of Eq. (5) between the boundaries E_n and E_x of the shock wave field along the ray trajectory yields

$$\beta = \frac{1}{n_0}\int_{E_n}^{E_x}\frac{\partial n}{\partial y}\mathrm{d}s \tag{6}$$

In the paraxial approximation $\beta = \frac{1}{n_0}\int_{E_n}^{E_x}\frac{\partial n}{\partial y}\mathrm{d}x$ (7)

In the system with axial symmetry, $r = (x^2 + y^2)^{1/2}$, and Eq. (7) become

$$\beta(y) = \frac{2y}{n_0}\int_y^R \frac{\partial n(r)}{\partial r}\frac{\mathrm{d}r}{(r^2 - y^2)^{1/2}} \tag{8}$$

The inversion of Eq. (8) is equivalent to the forward Abel transform

$$n(r) = n_0 - \frac{n_0}{\pi}\int_r^R \frac{\beta(y)}{(y^2 - r^2)^{1/2}}\mathrm{d}y \tag{9}$$

It can be seen from the Eq. (9), that for a definite detecting position r, the refraction index $n(r)$ will only be the function of R, which is the shock wave transmission radius. There will be

$$\frac{\mathrm{d}n(r)}{\mathrm{d}t} = -\frac{n_0}{\pi}\frac{\mathrm{d}n(r)}{\mathrm{d}R}\frac{\mathrm{d}R}{\mathrm{d}t} = -\frac{n_0}{\pi}v\frac{\beta(R)}{(R^2 - r^2)^{1/2}} \tag{10}$$

where v is the velocity of the shock wave front, R is only the function of t, and β is also the function of t, that is $\beta = \beta(R) = \beta(t)$. Combining Eq. (4), Eq. (10) becomes

$$\frac{\mathrm{d}n(r)}{\mathrm{d}t} = -\frac{n_0}{\pi}v\frac{\beta(t)}{(R^2 - r^2)^{1/2}} = -\frac{n_0}{\pi}v\frac{kI}{(R^2 - r^2)^{1/2}} \tag{11}$$

The constraint condition of Eq. (11) is $\mathrm{d}n(r)/\mathrm{d}t = 0$, if $R \leqslant r$. According to Eq. (11), the refraction index changing rate at radius r can be determined experimentally.

2 Experimental setup and results

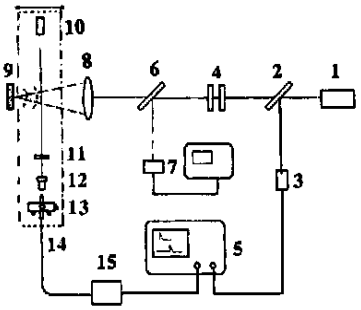

Fig. 3 The schematic diagram of the measurement system

The experimental system is shown in Fig. 3. 1—Q-switched Nd: YAG laser; 2—beam splitter; 3—PIN photodiode; 4—attenuator group; 5—oscilloscope; 6—beam splitter; 7—laser energy meter; 8—convex lens; 9—target; 10—He-Ne laser; 11—1064nm mirror; 12—microscope objecter; 13—5-axis fiber chuck positioner; 14—optical fiber; 15—photomultiplier. It consists of a shock wave generation module and a detection module. The shock wave generation module includes a Nd: YAG laser (200mJ, 1064nm, 12ns), two beam splitters, an attenuator group, a convex lens (with focal length of 14cm), a two-dimensional movable target, a PIN photoelectric diode (with 100ps rising edge) and an energy meter (Molectron EPM1000). The detection module includes a He-Ne laser (632. 8nm, 5mW), a microscope objective ($20^{\times}$), a fiber chuck positioner with 5 axes (0. 1μm position resolution), a single-mode fiber (for 632. 8nm), a photomultiplier (2ns rise time), and a digital oscilloscope (Tektronix THS730A, 1GS/s).

A high power laser pulse generated by the Nd: YAG laser 1 is partially reflected into a PIN photodiode 3 by the beam splitter 2 to give a steady electric pulse, which is fed into the oscilloscope 5 as the triggering signal to start sampling. To obtain the testing laser beam with suitable energy, an attenuator group 4 is inserted in the path of the transmitted pulse from the beam splitter. The laser pulse reflected from beam splitter 6 is monitored by the laser energy meter 7. The lens 8 focuses the transmitted laser pulse on the movable target (polished aluminum in this experiment), and induces the LPSW around the focal spot.

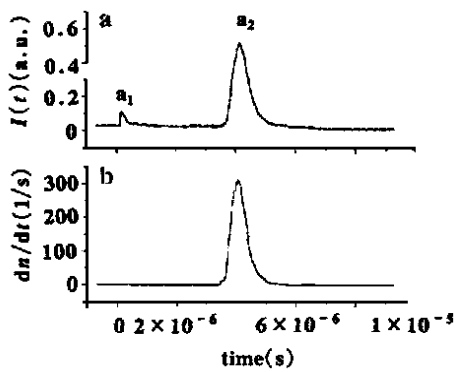

Fig. 4 A typical shock wave signal at r = 4mm away from the target (a); and the refractive index changing rate (b)
a—a_1 laser plasma flash; a_2 laser plasma shock wave deflection signal

The detection laser beam parallel with the target surface transmits through the 1064nm mirror 11, which reduces the influence of the laser pulse scattered by the plasma, and is coupled into the fiber 14 by the objective 12. The working point of the detection system is adjusted at point A with the positioner 13 as shown in Fig. 2. The beam deflection induced by LPSW is transformed into an electric pulse by the photomultiplier 15 and fed into the oscilloscope. The detection module, as indicated by the dash line frame in Fig. 3, is movable and has a spatial resolution up to 0. 02mm.

Fig. 4a shows a typical shock wave signal induced by a laser pulse of 200mJ at r = 4mm away from the target, and Fig. 4b the calibrated refractive index changing rate according to Eq. (11). It can be easily seen that the two peaks have similar shapes. This can be demonstrated from Eq. (11), which can be transformed into a series as

$$\frac{\mathrm{d}n(r)}{\mathrm{d}t} = -\frac{n_0}{\pi}\nu_s I(t)\left(\frac{1}{R} + \frac{1}{2}\frac{r^3}{R^3} + \frac{3}{8}\frac{r^4}{R^5} + \frac{5}{16}\frac{r^6}{R^7} + \cdots\right) \tag{12}$$

The series part of Eq. (12) converges quickly as the shock wave transmits. Here, we have assumed that ν is a constant when the shock wave front passing through the detection beam.

3 Discussion and conclusions

The refractive index may be gained from integrating Eq. (11) and this is 1.0005 at r = 4mm when the shock wave passing by. It is very close to the theoretical value 1.0006 calculated with the Gladstone-Dale formula. The refractive index at other position may be measured in the same way. The largest corresponding deflection angle in Fig. 4 is 3.6 mrad. It is in the linear deflection region that is less than 5 mrad.

Although PZTs are the most sensitive detectors available, piezo-electric ceramics generally suffer from being highly resonant detectors, and have a poor acoustic match to gases. The electric signals obtained from such detectors are strongly influenced by the properties of the detectors themselves. The fiber shock wave sensor offers a broadband, non-contact detection scheme, which allows the changing rate of the refractive index of the shock wave to be measured experimentally.

Based on the principle of the optical fiber sensor, it can be deduced that the cutoff frequency ν_c is linked to the rise time t_A of the photomultiplier by[11] $\nu_c = 1/2t_A$. Under our experimental conditions, accordingly, a pulse of up to 250MHz frequency can be detected without any distortion. The bandwidth can be broadened with a faster response photomultiplier. The sensitivity is determined by the size of the detection beam waist w, the objective focal length f, the fiber core diameter, and the detection laser wavelength. Eq. (1) indicates that a smaller beam waist, a longer objective focal length, a smaller core diameter fiber, and a shorter laser wavelength are beneficial for improving the sensitivity of the sensor. However, the measuring range will decrease accordingly. The principle of the sensor does not set the limitation to the media, so applications requiring a broadband measurement of shock waves or intensive acoustic pulse in gas or other transparent media are envisaged as being appropriate for this technique, especially in cases where a non-contact measurement is important.

Acknowledgements

This work was supported by the "Trans-Century Training Program Foundation for the Talents by the State Education Communication", the "Fok Ying Tung Education Foundation" and the "Nature Science Foundation of Jiangsu Province"(China). The authors are grateful for helpful discussion with doctor W. Yao.

References

1 Ni X W, Lu J, He A Z *et al*. Opt Commun, 1989; 74: 185
2 Callies G, Berger P, Kastle J *et al*. SPIE, 1995; 2502: 706

激光微束细胞操作系统*

李 岩[a] 张书练[a] 孟祥旺[a] 张志诚[b] 欧家鸣[c] 刘静华[a]
([a]清华大学精密测试技术与仪器国家重点实验室, 北京, 100084)
([b]清华大学生物膜与膜生物国家重点实验室, 北京, 100084)
([c]云南师范大学物理系, 昆明, 650092)

摘要: 提出构建一种用于生物细胞操作的激光微束系统。即由 Nd: YAG 激光经物镜聚焦形成的光刀和 He-Ne 激光器经物镜聚焦形成的光镊组成的激光微束系统, 进行了总体设计、关键部件设计和选择。在构建的激光微束操作实验系统上实现了非接触细胞操作, 验证了光镊的力学效应。采用 Nd: YAG 经显微物镜会聚形成光刀可以对细胞或细胞器进行打孔或切割染色体。

关键词: 激光微束 光刀 光镊 细胞操作

A laser micro-beam system for cell manipulation

Li Yan[a], *Zhang Shulian*[a], *Meng Xiangwang*[a], *Zhang Zhicheng*[b], *Ou Jiaming*[c], *Liu Jinghua*[a]
([a] State Key Laboratory of Precision Measurement Technology and Instruments, Tsinghua University, Beijing, 100084)
([b] State Key Laboratory of Biomembrane & Membrane Biotechnology, Tsinghua University, Beijing, 100084)
([c] Department of Physics, Yunnan Normal University, Kunming, 650092)

Abstract: A laser mire-beam system for cell manipulation is introduced in the paper. It consists of an optical scalpel, which is a Nd: YAG laser beam focused tightly by an objective and an optical trap, the focused He-Ne laser beam. Not only the overall design of the laser micro-beam system but also the design and the choice of the critical components of the system are reviewed. The optical trap can manipulate cells in suspension, it validates the kinetic performance of the laser trap. The optical scalpel can concise chromosome and punch holes in cells or organelles.

* 北京市自然科学基金和清华大学基础研究基金资助。

3 Kurniawan H, Budi W S, Suliyanti M M *et al*. J Phys D: Appl Phys, 1997; 30: 3335
4 Kurniawan H, Ishikawa Y, Nakajima S *et al*. Appl Spectrosc, 1997; 51: 1769
5 Mahdieh M H, Hall T A. J Phys D: Appl Phys, 1997; 30: 588
6 Ni X W, Zhou B, Chen J P *et al*. Acta Physica Sinica (Overseas edition), 1998; 2: 143
7 Ni X W, Chen J P, Shen Z H *et al*. International J of Optoelectronics, 1998; 12: 37
8 Depaula R P, Flax L, Cole J H *et al*. IEEE J Q E, 1982; QE18(4): 213
9 Chen J P, Ni X W, Lu J *et al*. Progress in Natural Science, 1996; A supplement to vol 6: s-425
10 Chen J P, Ni X W, Lu J *et al*. SPIE, 1996; 2895: 208
11 Vogel A, Lauterorn W. J Acoust Soc Amer, 1988; 84: 719
12 Siano S, Pacini G, Pini R *et al*. Optics Commun, 1998; 154: 319
13 Bar-Ziv E, Sgulim S, Kafri O *et al*. Appl Opt, 1983; 22: 5
14 Marcuse D. Light Transmission Opt. New York: Van Nostrand, 1972

* * *

作者简介: 陈建平, 男, 1967 年 12 月出生。博士生。现从事激光对材料的破坏机理和测试技术研究。

收稿日期: 1999-09-20 收到修改稿日期: 1999-12-07